FAST SYNTHESIS OF HIGHLY STABLE ZnO-Co^{2+} DOPED CERAMIC PIGMENTS: A QUICK AND SIMPLE APPROACH

Gleison N. Marques[1]*, Dayana A Cunha[2], Thayane P. Oliveira[1], Naldirene N. Fonseca[3], Geraldo E. Luz Júnior[4], Andrea D. N. Lago[5], Marcelo M. Oliveira[1,2], Maria I. B. Bernardi[6], Emilio Azevedo[2]

1 - Programa de Pós-graduação em Engenharia de Materiais - PPGEM, Instituto Federal de Educação, Ciência e Tecnologia do Maranhão (IFMA), Sao Luis, MA, Brasil.
2 - Departamento de Química (DAQ), Instituto Federal de Educação, Ciência e Tecnologia do Maranhão (IFMA), São Luís, MA, Brasil.
3 - Programa de Pós-graduação em Química - PPGQ, Instituto Federal de Educação, Ciência e Tecnologia do Maranhão (IFMA), São Luís, MA, Brasil.
4 - Programa de Pós-graduação em Química - (PPGQ-CCN-GERATEC), Universidade Estadual do Piauí (UESPI), Teresina, PI, Brasil.
5 – Departamento de Odontologia – Universidade Federal do Maranhão, São Luís, MA, Brasil.
6 – Instituto de Física de São Carlos (IFSC), Universidade de São Paulo (USP), São Carlos, SP, Brasil.

gleison@estudante.ufscar.br

ABSTRACT

In this work, we report on the development of single-phase ceramic powders with excellent thermal and colorimetric stability using the sol-gel combustion method for the production of zinc oxide doped with Co^{2+} ($Zn_{1-x}Co_xO$; x= 0.0, 0.04, 0.1, and 0.2 mol). The techniques of X-ray diffraction (XRD), high-resolution scanning electron microscopy (SEM-FEG), X-ray dispersive spectroscopy (EDS), and UV-Vis spectroscopy (UV-Vis) were used to characterize the pigments produced. The XRD patterns of the samples heat-treated at 1000 ºC/2h indicated obtaining single-phase powders, confirmed by the Rietveld refinement. The pigments showed agglomerated particles with an almost spherical shape. CIELab measurements showed that pigments modified with 10 and 20% cobalt, subjected to heat treatment up to 1000 ºC, showed better values of the a coordinate, thus indicating the formation of a green pigment with better tonality.*

Keywords: *Ceramic pigments. Sol-gel combustion method. CIELab colorimetric parameters.*

INTRODUCTION

Zinc oxide (ZnO) is an *n*-type semiconductor with a wide bandgap (3.4 eV), extensively studied for applications in several areas [1]. Several strategies have been studied to improve the properties of ZnO, such as modifying this matrix by adding transition metal ions [1]. The doping of ZnO using cobalt ($Zn_{1-x}Co_xO$) presents itself as an exciting alternative for synthesizing green pigments with excellent thermal stability to replace the use of chromium [2] because the valence

of the Zn^{2+} ion can be assumed by metals with an incomplete 3d orbital, facilitating the replacement of the Co^{2+} ion in the Zn^{2+} sites [3].

There are several ways in the literature by which $Zn_{1-X}Co_xO$ can be obtained, such as the synthesis by co-precipitation, solid-state reaction, and combustion synthesis [4,5]. Among these, combustion synthesis (CS) stands out as a sustaining autonomous method where the reactants quickly and efficiently heat the reaction medium, producing pure and homogeneous materials for applications in several areas [6,7]. The main advantages of this technique are the rapid processing of the synthesis and the possibility of obtaining a variety of metallic oxides [8]. Thus, this work produced single-phase ceramic pigments based on zinc oxide doped with different concentrations of cobalt ($Zn_{1-x}Co_xO$; x = 0, 0.04, 0.1 and 0.2 mol) by the CS method without using mineralizers. The effects of cobalt doping on the pigments' structural, optical, and morphological properties were also evaluated.

MATERIALS AND METHODS

2.1 Pigment synthesis

In the synthesis of $Zn_{1-X}Co_xO$ ceramic powders (x = 0, 4, 10, and 20% mol), zinc nitrate ($Zn(NO_3)_2.6H_2O$ – Synth – 98%) and cobalt nitrate were used ($Co(NO_3)_2.6H_2O$ – Synth – 99%) as metallic precursors, while the fuel chosen was urea ($CO(NH_2)_2$ – Synth – 98%). The oxidant/fuel ratios were defined according to the total valence of the nitrates and the fuel that act as oxidants and reductants in the reaction, respectively. The mass of zinc nitrate, cobalt nitrate, and urea (g) needed to synthesize the pure samples was 3.12, 0.0, and 1.02, respectively. For synthesizing the samples doped with 4%.mol Co, 3.06, 0.30, and 2.03 were used, respectively. To synthesize the materials doped with 10 %.mol Co, 3.09, 0.75, and 20%.mol, 2.06, 3.05, 0.9, and 3.07 were used, respectively.

Initially, the nitrates were solubilized with distilled water (20 mL) in a beaker and kept under constant stirring and heating (80 °C). The urea was added to the solution after the complete homogenization of the nitrates. The temperature was kept constant until the evaporation of a large part of the solvent occurred, resulting in the formation of a gel, as shown. Then, the beaker was taken to a muffle furnace previously heated to 400 °C and kept for 30 min (rate 10 ºC/min) to initiate the auto-ignition process and subsequent combustion. The powder resulting from the reaction was de-agglomerated in an agate mortar and heat-treated at 1000 °C for 2h (rate 10 ºC/min). For ease of understanding, the samples have been labeled ZnO – 1 (400 ºC/30 min), ZnO – 2 (1000 ºC/2 h), ZnO – 3 (4%.mol Co – 400 ºC/30 min), ZnO – 4 (4%.mol Co – 1000 ºC/2 h), ZnO – 5 (10%.mol Co – 400 ºC/30 min), ZnO – 6 (10%.mol Co – 1000 ºC/2 h), ZnO – 7 (20%.mol Co – 400 ºC/30 min), and ZnO – 8 (20%.mol Co – 1000 ºC/2 h).

2.2 Characterizations

The powders produced were characterized by X-ray diffraction (XRD) using a Shimadzu Lab XRD 6100 diffractometer, 2θ scan in the range of 10-80°, with CuKα radiation (λ = 1.5418 Å). Crystallite sizes were obtained using Scherrer and Williamson-Hall equations [9]. The structural refinement of the material phases was performed using the Rietveld Method with the GSAS software (General Structure Analysis System program) with the EXPGUI interfaces [10]. The morphology of the samples was analyzed using a Scanning Electron Microscope with a field emission electron beam and coupled to an Energy Dispersive Spectrometer (SEM-FEG-EDS) model FEG Quanta 450. The UV-Vis diffuse reflectance measurements were obtained

using a model UV-2600 spectrophotometer (Shimadzu, Japan) with a wavelength of 200 to 800 nm. The color of the pigments and coatings produced was determined with the aid of a GRETAGMACBETH COLOR-EYE 2180 spectrophotometer, equipped with a standard light source type D65 (daylight) corresponding to CIELab (Commission Internationale de l'Eclairage) standards [11]. Through this technique, one can accurately obtain the coordinates referring to the color of the material in the three-dimensional space CIELab, where L represents the luminosity (L* = 100 white and 0 black), the* axis the red-green colors (a* positive = red, a* negative = green) and the b* axis associated with the yellow-blue colors (b* positive = yellow, b* negative = blue).

RESULTS AND DISCUSSION

X-ray diffractograms of samples $Zn_{1-x}Co_xO$ with x = 0, 4, 10, and 20% mol, obtained after combustion at 400 °C/30 min and after heat treatment at 1000 °C/2h, are shown in Fig. 1. The diffraction peaks of the samples correspond to the Wurtzite phase, which has a hexagonal crystal system and P63mc space group (JCPDS 75-0576).

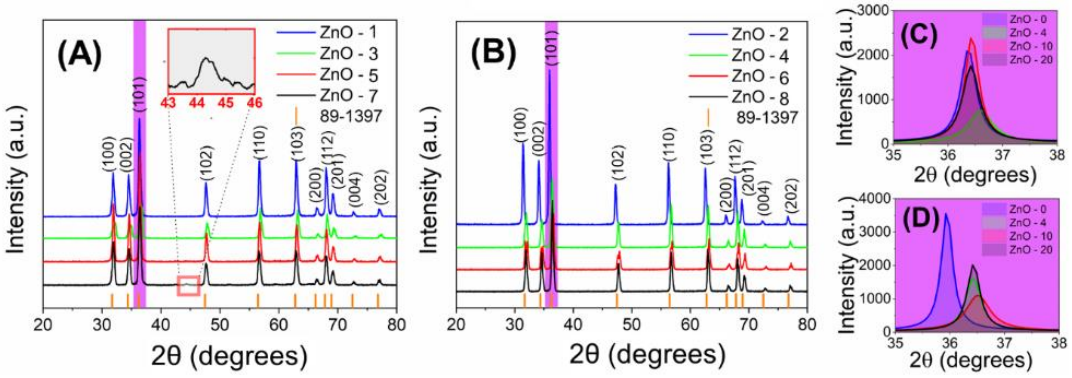

Fig. 1: XRD of cobalt-modified ZnO pigments: (a) obtained after combustion at 400 °C/30 min, (b) calcined at 1000 °C/2h, (C) and (D) increase in the region corresponding to the peak of diffraction with greater intensity of each group of samples.

The diffractograms of the samples modified with 10 and 20% cobalt still show a small diffraction peak around 44º (2θ) corresponding to the secondary phase Co (JCPDS 01-1255), possibly related to the considerably fast synthesis time. Through the profiles of the diffraction peaks of the samples treated at 1000 ºC/2h, it is possible to observe an increase in crystallinity and the disappearance of the secondary phase, both influenced by the rise in the thermal treatment temperature of powders. Mandal et al. [12] observed that impurity peaks are strongly associated with doping above 30%. Despite this, Pragna et al. and Hoang et al. [13,14] reported the formation of secondary phases in powders produced in less than 10% contractions. Zhou et al. [8] investigated the effect of different fuels on the combustion process (glycine and urea) of ZnO powders doped with 4% cobalt. Other studies have shown the presence of secondary Co_3O_4 phases even when using high heat treatment temperatures [15]. Regarding the most intense diffraction peak (101), observed in the two groups of samples (400 and 1000 ºC) and represented in Fig. 1.c-d, it is possible to notice a variation in their positions for increasing values concerning 2θ, mainly in samples treated at 1000 ºC/2h. This behavior evidences the replacement of Zn^{2+} by Co^{2+} due to the ionic radius values being very close to 0.058 nm and 0.060 nm, respectively [16].

The X-ray diffraction profiles fit the theoretical model (CIF 65119) and the experimental data. Furthermore, this agreement is because we used a pseudo-Voigt profile function [17], which solves the convolution of the peaks using an approximation between Gaussian and Lorentzian functions. The data obtained through the Rietveld refinement of the heat-treated samples at 1000 °C/2h and the agreement factors of the fit between the observed and calculated profiles ($\chi^2 e$ *WRp*) are presented in Table 1. Upon analyzing the table, it has been confirmed that a notable contrast exists between the pure sample's network parameters and the values of the altered powders. It is also noted that parameters *a* and *c* increase as higher concentrations of the dopant are added to the network, indicating, once again, the replacement of Zn^{2+} by Co^{2+}. These values range from 3.250 to 3.251 Å (a) and 5.207 to 5.2519 Å.

Table 1: Structural parameters (*a* and *c*), unit cell volume, the goodness of fit factors (X^2 *e wRp)* obtained through Rietveld refinement and crystallite sizes calculated using the Williamson-Hall (W-H) and Scherrer (S) equations.

Co^{2+} (% mol)	Lattice parameters						Crystallite size /nm (*D*)	
	***a* (Å)**	***c* (Å)**	***c*/*a* (Å)**	***Volume* (Å³)**	**χ^2**	***wRp***	**W-H**	**S**
0.00	3.250	5.207	1.601	47.657	2.94	0.13	26.46	27.31
0.04	3.249	5.199	1.599	47.563	2.99	0.25	15.24	23.13
0.10	3.250	5.201	1.600	47.609	1.93	0.17	24.11	26.53
0.20	3.251	5.251	1.615	47.659	2.22	0.19	19.37	22.94

In comparison with the unit cell of the pure material, it is observed that the volumes presented for the doped samples are larger. The unit cell expansion observed in the refinement may indicate the presence of interstitial atoms generated with the increase of the percentage of dopant that also increases the crystallite size, as verified through the calculations of *D* (Table 1). In addition, there is an increase in crystallite size values as a function of heat treatment. Regarding the modification of the cell's lattice parameters by the addition of cobalt, there is a decrease in crystallite size between the samples with 10 and 20% mol, which may be associated with lower nucleation of Zn atoms with the addition of higher concentrations of the dopant [18].

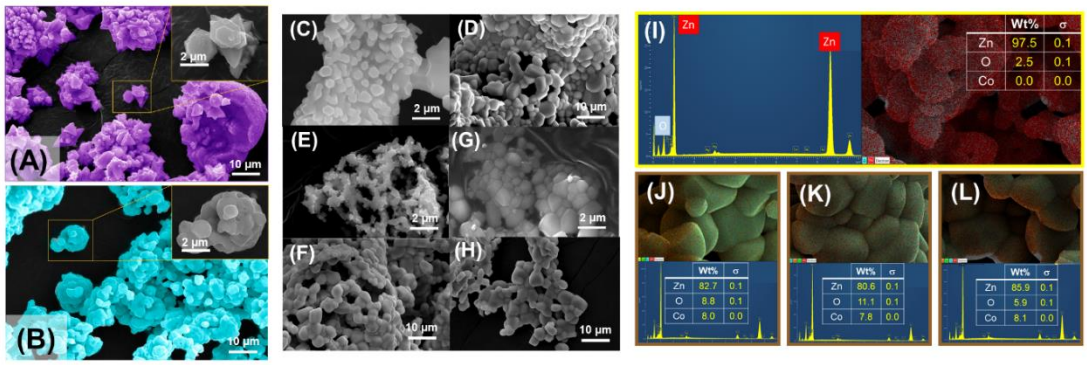

Fig. 2: SEM images of (a) ZnO -1, (b) ZnO – 2 (c) ZnO – 3, (d) ZnO – 4, (e) ZnO – 5, (f) ZnO – 6, (g) ZnO - 7, (h) ZnO – 8, and EDS spectrum of the samples (i) ZnO – 2, (j) ZnO – 4, (k) ZnO – 6, and (l) ZnO – 8.

SEM-FEG analyzed the morphologies of the particles, and the results are shown in Fig. 2. The pure ZnO sample (Fig. 2a), obtained after the combustion process, presents a morphology of

faceted pyramids with a hexagonal base. These particles tend to agglomerate from the edges, forming flower-shaped micro-agglomerates, as can be seen in the magnification in Fig. 2a. On the other hand, the powders that underwent heat treatment show the sintering of very agglomerated semi-spherical particles (Fig. 2b). Co^{2+} modified pigments (Fig. 2c-h) also exhibit strongly agglomerated particles with a slightly spherical and non-uniform shape, mainly in samples heat-treated at 1000 ºC/2h. In addition to being strongly agglomerated, the sample doped with 4% Co^{2+} (400 ºC) also exhibits a hexagonal base, similar to the morphology seen in the pure sample obtained at the same temperature.

On the other hand, the doped samples subjected to heat treatment at 1000 ºC/2h present larger particles with faceted morphology with different shapes. Previous studies have also reported the production of ZnO particles doped with Co by other methods and with almost spherical morphologies [19]. Regarding the effect of heat treatment on non-doped pigments, there is a slight decrease in the average particle size from 0.97 µm (400 ºC/30min) to 0.95 µm (1000 ºC/2h). The particle sizes of samples doped with 4 and 10 %mol of Co (1000 ºC/2h) showed a particle size of 2.23 and 2.07 µm. Energy dispersive X-ray (EDX) analysis of heat-treated powders at 1000 °C/2h (Fig. 2i-l) demonstrates the purity of the ZnO sample without incorporating Co^{2+}, where only the elements of interest, Zn and O, are observed. The spectra of the samples doped with cobalt and the atomic compositions presented in the tables show the presence of Co^{2+} in the produced pigments (Fig. 2.j-l).

Fig. 3 shows the reflectance spectra of pure and Co-modified ZnO samples. The samples obtained after combustion (Fig. 3a) present absorption peaks at 537 nm, 565 nm, and 610 nm, which increase their reflectance according to the content of Co^{2+} inserted in the structure and are close to the values reported by Sutka et al. [3] (569 - $^4A_2(F) \rightarrow {}^2A_1(G)$ e 612 - $^4A_2(F) \rightarrow {}^4T_1(P)$). Xie et al. [20] and Ji et al. [21] observed similar peaks in the spectra obtained from the doping of ZnO by Co. They associated them with the electronic transitions $^4A_2(F) \rightarrow {}^2A_1(G)$ (565 nm) e $^4A_2(F) \rightarrow {}^2T_1(P)$ (610 nm), respectively, considering the diagrams for Co^{2+} in a tetrahedral coordination environment (d^7; T_d), according to the Tanabe-Sugano diagram. These characteristic peaks indicate the substitution of Zn^{2+} by Co^{2+} in the ZnO lattice.

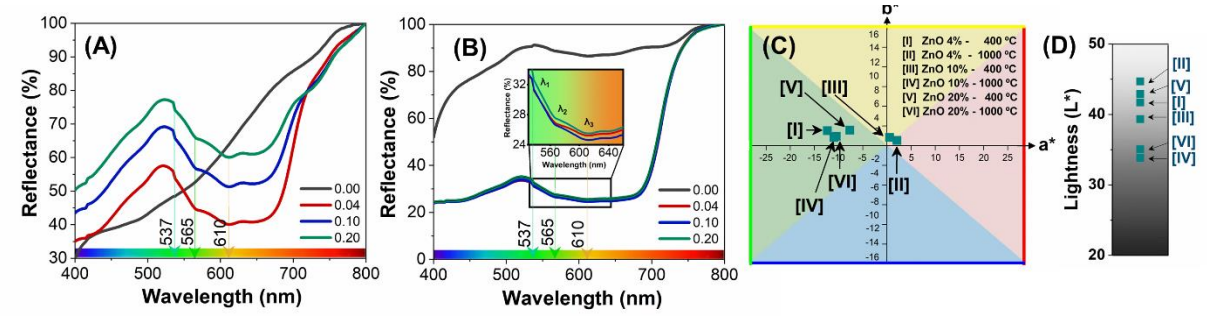

Fig. 3: Reflectance spectra for pure and Co-doped samples treated at (a) 400 °C/ 30 min, (b) 1000 °C/2 h, and CIELab diagrams of the produced pigments showing the (c) parameter a* versus b*, (d) luminosity parameter, L.

The colorimetric characteristics of the pigments were analyzed using the three-dimensional CIELab color space coordinates using a light source (D65-10°) and standardized by the International Commission on Illumination (CIE). The negative values of the parameter of a*(Fig. 3c), which represents the green portion of the CIELab color chart, for samples modified with 10 and 20% Co and heat-treated at 1000 ºC, indicate that temperature plays a

vital role in increasing the tone of the pigments. Among the pigments produced, the one that presented the highest value of the a* coordinate and, therefore, the best green hue was the sample modified with 4% cobalt, obtained after the synthesis process (a* = -12.32). Furthermore, it is observed that the pigments obtained after heat treatment at 1000 ºC show an increase in green color as higher concentrations of the dopant are added to the ZnO structure - 7.33 (4%), -10.49 (10%), and -10.95 (20%), respectively. The luminosity is also significantly affected by the increase in temperature and the concentrations of dopant, as can be seen from the darkening of the powders indicated by the decrease in the parameter L (Fig. 3d). Zhou et al. [15] also observed similar behavior concerning reducing the luminosity of the Co-doped ZnO powders produced by the combustion method. They associated this with the increase in the size of the particles in the pigments.

CONCLUSIONS

This work used the sol-gel combustion method to produce cobalt-doped zinc oxide pigments using different concentrations. The replacement of Zn^{2+} by Co^{2+} was evidenced by the increased lattice parameters obtained by the Rietveld refinement and the transition bands observed in the UV-Vis spectra. The morphology of the powders, analyzed by SEM-FEG, revealed the formation of powders with a faceted pyramid geometry with a hexagonal base for the undoped ZnO sample (400 ºC). In contrast, the calcined models at 1000 ºC/2h were strongly clustered and almost spherical. The colorimetric analysis of the pigments heat-treated at 1000 ºC/2h showed a green color depending on the temperature and the dopant content. The luminosity of the powders was strongly affected by the increase in temperature, as evidenced by the decrease in L values.

ACKNOWLEDGMENTS

The authors are grateful for the financial support provided by the Federal Institute of Maranhão, CAPES, CNPq, FAPEMA (BIC-03384/15 and BIC-05159/16), FAPESP (CDMF 2013/07296-2), Central Analítica-UFC (funded by Finep-CT-INFRA, CAPES – Pró-Equipamentos, and MCTI-CNPq-SisNano2.0) for microscopy measurements.

REFERENCES

[1] FAN, Y. XU, Y. WANG, Y. SUN, Y. Fabrication and characterization of Co-doped ZnO nanodiscs for selective TEA sensor applications with high response, high selectivity and ppb-level detection limit, J Alloys Compd. 876 (2021) 160170.

[2] ZHOU, N. ZHANG, Y. NIAN, S. LI, W. LI, J. CAO, W. WU, Z. Synthesis and characterization of Zn1-xCoxO green pigments with low content cobalt oxide, J Alloys Compd. 711 (2017) 406–413.

[3] ŠUTKA, A. KÄÄMBRE, T. PÄRNA, R. JUHNEVICA, I. MAIOROV, M. JOOST, U. KISAND, V. Co doped ZnO nanowires as visible light photocatalysts, Solid State Sci. 56 (2016) 54–62.

[4] NAIK, E.I. BHOJYA NAIK, H.S. SARVAJITH, M.S. PRADEEPA, E. Co-precipitation synthesis of cobalt doped ZnO nanoparticles: Characterization and their applications for biosensing and antibacterial studies, Inorg Chem Commun. 130 (2021) 108678.

[5] GODAVARTI, U. MOTE, V.D. DASARI, M. Role of cobalt doping on the electrical conductivity of ZnO nanoparticles, Journal of Asian Ceramic Societies. 5 (2017) 391–396.

[6] OLIVEIRA, T.P. MARQUES, G.N. MACEDO CASTRO, M.A. VIANA COSTA, R.C. RANGEL, J.H.G. RODRIGUES, S.F. DOS SANTOS, C.C. OLIVEIRA, M.M. Synthesis and photocatalytic investigation of $ZnFe_2O_4$ in the degradation of organic dyes under visible light, Journal of Materials Research and Technology. 9 (2020)

[7] MARQUES, G.N. OLIVEIRA, T.P. TEIXEIRA, M.M. LOT, A.V. DO NASCIMENTO, M.F. RANGEL, J.H.G. AZEVEDO, E. RODRIGUES, S.F. BERNARDI, M.I.B. LONGO, E. OLIVEIRA, M.M. Synthesis of yttrium aluminate doped with Cr^{3+} using MgF_2–$Na_2B_4O_7$ as mineralizers to obtain red pigments for ceramic tiles application, Ceram Int. 46 (2020) 27940–27950.

[8] TAO, K. ZHOU, S. ZHANG, Q. KONG, C. MA, Q. TSUBAKI, N. L. Chen, Sol-gel auto-combustion synthesis of Ni-$Ce_xZr_{1-x}O_2$ catalysts for carbon dioxide reforming of methane, RSC Adv. 3 (2013) 22285–22294.

[9] MUSTAPHA, S. NDAMITSO, M.M. ABDULKAREEM, A.S. TIJANI, J.O. SHUAIB, D.T. MOHAMMED, A.K. SUMAILA, A. Comparative study of crystallite size using Williamson-Hall and Debye-Scherrer plots for ZnO nanoparticles, Advances in Natural Sciences: Nanoscience and Nanotechnology. 10 (2019) 045013.

[10] TOBY, B.H. EXPGUI, a graphical user interface for GSAS Applied Crystallography, J. Appl. Cryst. 34 (2001) 210–213.

[11] BILLMEYER, F.W. FAIRMAN, H.S. CIE Method for Calculating Tristimulus Values, Color Res Appl. 12 (1987) 27–36.

[12] MANDAL, S.K. DAS, A.K. NATH, T.K. KARMAKAR, D. Temperature dependence of solubility limits of transition metals (Co, Mn, Fe, and Ni) in ZnO nanoparticles, Appl Phys Lett. 89 (2006) 144105.

[13] PRAGNA, E. RAMANADHA, M. SUDHARANI, A. KUMAR, K.S. Nano Synthesis and Characterization of Co and Mn Co-doped ZnO by Solution Combustion Technique, J Supercond Nov Magn. 34 (2021) 1507–1516.

[14] HOANG, L.H. VAN HAI, P. HAI, N.H. VAN VINH, P. CHEN, X.B. YANG, I.S. The microwave-assisted synthesis and characterization of $Zn_{1-x}Co_xO$ nanopowders, Mater Lett. 64 (2010) 962–965.

[15] ZHOU, N. LUAN, J. ZHANG, Y. LI, M. ZHOU, X. JIANG, J. TANG, F. Synthesis of high near infrared reflection wurtzite structure green pigments using Co-doped ZnO by combustion method, Ceram Int. 45 (2019) 3306–3312.

[16] ALI, R.N. NAZ, H. LI, J. ZHU, X. LIU, P. XIANG, B. Band gap engineering of transition metal (Ni/Co) codoped in zinc oxide (ZnO) nanoparticles, J Alloys Compd. 744 (2018) 90–95.

[17] THOMPSON, P. COX, D.E. HASTINGS, J.B. Rietveld refinement of Debye–Scherrer synchrotron X-ray data from Al_2O_3, J Appl Crystallogr. 20 (1987) 79–83.

[18] CHATTOPADHYAY, S. MISRA, K.P. AGARWALA, A. SHAHEE, A. JAIN, S. HALDER, N. RAO, A. BABU, P.D. SARAN, M. MUKHOPADHYAY, A.K. Dislocations and particle size governed band gap and ferromagnetic ordering in Ni doped ZnO nanoparticles synthesized via co-precipitation, Ceram Int. 45 (2019) 23341–23354.

[19] BIRAJDAR, S.D. KHIRADE, P.P. SARAF, T.S. ALANGE, R.C. JADHAV, K.M. Sol-gel auto combustion synthesis, electrical and dielectric properties of Zn1−xCoxO ($0.0 \leq x \leq 0.36$) semiconductor nanoparticles, J Alloys Compd. 691 (2017) 355–363.

[20] XIE, F. GUO, J.-F. WANG, H.-T. CHANG, N. Enhancing visible light photocatalytic activity by transformation of Co^{3+}/Co^{2+} and formation of oxygen vacancies over rationally Co doped ZnO microspheres, Colloids Surf A Physicochem Eng Asp. (2021) 128157.

[21] JI, H. CAI, C. ZHOU, S. LIU, W. Structure, photoluminescence, and magnetic properties of Co-doped ZnO nanoparticles, 29 (2018) 12917–12926.